UC Berkeley
Archaeological X-ray Fluorescence Reports

Title

SOURCE PROVENANCE OF ARCHAEOLOGICAL OBSIDIAN FROM ARCHAEOLOGICL SITES ALONG THE RIO SANTA MARIA, CENTRAL CHIHUAHUA

Permalink

https://escholarship.org/uc/item/31b0t3dk

Author

Shackley, M. Steven

Publication Date

2018-09-07

eScholarship.org Powered by the California Digital Library
University of California

GEOARCHAEOLOGICAL XRF LAB
A GREEN SOLAR FACILITY

GEOARCHAEOLOGICAL X-RAY FLUORESCENCE SPECTROMETRY LABORATORY (www.swxrflab.net)
8100 WYOMING BLVD., SUITE M4-158 ALBUQUERQUE, NM 87113 USA

SOURCE PROVENANCE OF ARCHAEOLOGICAL OBSIDIAN FROM ARCHAEOLOGICL SITES ALONG THE RIO SANTA MARIA, CENTRAL CHIHUAHUA

Sample of obsidian projectile points from project sites. Site names followed by XRF lab #s, source assignments in italics. The projectile points would likely be considered a version of Late Archaic Cienega Phase points in Arizona and New Mexico (see Sliva 2015).

by

M. Steven Shackley, Ph.D., Director
Geoarchaeological XRF Laboratory
Albuquerque, New Mexico, USA

Report Prepared for

Dr. Emiliano Gallaga M.
Escuela Antropología e Historia del Norte de México
Chihuahua, Chih., México

7 September 2018

INTRODUCTION

The analysis here of 61 obsidian artifacts from sites along the Rio Santa Maria in central Chihuahua indicates a mix of sources from the secondary deposits along the Rio Santa Maria, the coalesced domes at Sierra Fresnal, and the Agua Fria/Sierra la Brena source along the Sonora/Chihuahua border in the northern Sierra Madre Occidental (see Shackley 2005; Figure 1 here). A number of, as yet, unlocated sources were also in the assemblage, but are likely from somewhere in northwest Mexico.

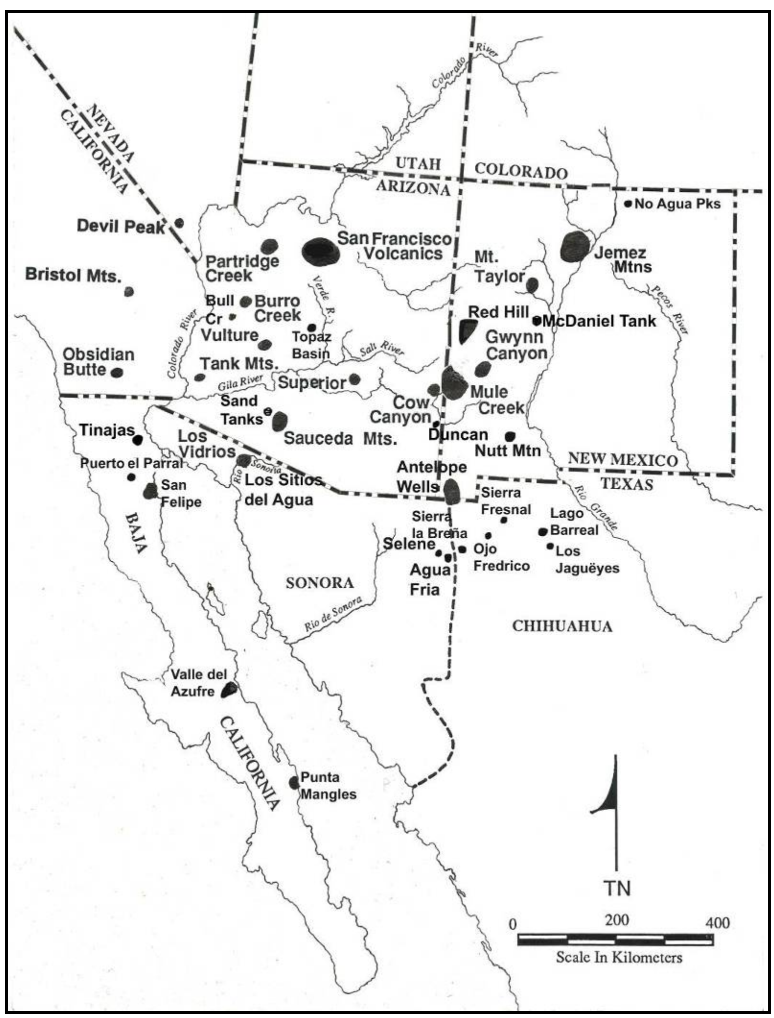

Figure 1. Approximate location of sources of archaeological obsidian in the North American Southwest (updated and adapted from Shackley 1989, 2005).

ANALYSIS AND INSTRUMENTATION

All archaeological samples are analyzed whole. The results presented here are quantitative in that they are derived from "filtered" intensity values ratioed to the appropriate x-ray continuum regions through a least squares fitting formula rather than plotting the proportions of the net intensities in a ternary system (McCarthy and Schamber 1981; Schamber 1977). Or more essentially, these data through the analysis of international rock standards, allow for inter-instrument comparison with a predictable degree of certainty (Hampel 1984; Shackley 2011).

All analyses for this study were conducted on a ThermoScientific *Quant'X* EDXRF spectrometer, located at the Geoarchaeological XRF Laboratory, Albuquerque, New Mexico. It is equipped with a thermoelectrically Peltier cooled solid-state Si(Li) X-ray detector, with a 50 kV, 50 W, ultra-high-flux end window bremsstrahlung Rh target X-ray tube and a 76 μm (3 mil) beryllium (Be) window (air cooled), that runs on a power supply operating from 4-50 kV/0.02-1.0 mA at 0.02 increments. The spectrometer is equipped with a 200 $l\ min^{-1}$ Edwards vacuum pump, allowing for the analysis of lower-atomic-weight elements between sodium (Na) and titanium (Ti). Data acquisition is accomplished with a pulse processor and an analogue-to-digital converter. Elemental composition is identified with digital filter background removal, least squares empirical peak deconvolution, gross peak intensities and net peak intensities above background.

Trace Element Analysis

The analysis for mid Zb condition elements Ti-Nb, Pb, Th, the x-ray tube is operated at 30 kV, using a 0.05 mm (medium) Pd primary beam filter in an air path at 100 seconds livetime to generate x-ray intensity $K\alpha_1$-line data for elements titanium (Ti), manganese (Mn), iron (as $Fe_2O_3^T$), cobalt (Co), nickel (Ni), copper, (Cu), zinc, (Zn), gallium (Ga), rubidium (Rb), strontium (Sr), yttrium (Y), zirconium (Zr), niobium (Nb), lead (Pb), and thorium (Th). Not all these elements are reported since their values in many volcanic rocks are very low. Trace element intensities were converted to concentration estimates by employing a linear calibration line ratioed to the Compton scatter established for each element from the analysis of international rock standards certified by the National Institute of Standards and Technology (NIST), the US. Geological Survey (USGS), Canadian Centre for Mineral and Energy Technology, and the Centre de Recherches Pétrographiques et Géochimiques in France (Govindaraju 1994). Line fitting is linear (XML) for all elements. When barium (Ba) is analyzed in the High Zb condition, the Rh tube is operated at 50 kV and up to 1.0 mA, ratioed to the bremsstrahlung region (see Davis 2011; Shackley 2011). Further details concerning the petrological choice of these elements in Southwest obsidians is available in Shackley (1988, 1991, 1995, 2005; c.f. Mahood and Stimac 1991; and Hughes and Smith 1993). Nineteen specific pressed powder standards are used for the best fit regression calibration for elements Ti-Nb, Pb, Th, and Ba, and include G-2 (basalt), AGV-2 (andesite), GSP-2 (granodiorite), SY-2 (syenite), BHVO-2 (hawaiite), STM-1 (syenite), QLO-1 (quartz latite), RGM-1 (obsidian), W-2 (diabase), BIR-1 (basalt), SDC-1 (mica schist), TLM-1 (tonalite), SCO-1 (shale), NOD-A-1 and NOD-P-1 (manganese) all US Geological Survey standards, NIST-278 (obsidian), U.S. National Institute of Standards and Technology, BE-N (basalt) from the Centre de Recherches Pétrographiques et Géochimiques in France, and JR-1 and JR-2 (obsidian) from the Geological Survey of Japan (Govindaraju 1994).

The data from the WinTrace software were translated directly into Excel for Windows and into SPSS ver. 21 and JMP 12.0.1 for statistical manipulation. The USGS rhyolite standard RGM-1 is analyzed during each sample run for obsidian artifacts to evaluate machine calibration (Table 1). Source assignments were made by reference to source data at http://swxrflab.net/swobsrcs.htm and Shackley (1995, 2005; Kibler et al. 2014; see also Fralik et al. 1998). Sample numbers (XRF #) are assigned by the laboratory and clearly marked on the ziploc bags for reference.

DISCUSSION

Two of the dominant sources here, Los Jagueyes and Sierra Fresnal are commonly recovered in archaeological contexts in northern Chihuahua and southern New Mexico (see Tables 1 and 2, Figures 2 and 3). The Sierra Madre source Agua Fria/Sierra la Breña, has not been recovered as commonly (see Shackley 2005:80-85, Appendix). Assuming these Archaic hunter-gatherers were relatively mobile, the obsidian source provenance indicates a procurement range that included the Sierra Fresnal area, and the Sierra Madre, in addition to the Rio Santa Maria valley. The Sierra Madre source area is an excellent resource for artiodactyls, piñon, and other subsistence foods, as well as obsidian raw material. The extent of secondary deposits from the Sierra Madre sources in unknown, but could have eroded downstream to the east or the west.

Source Discussion

The sources recovered from these Rio Santa Maria sites deserves some discussion. See also Shackley (2005:79-85).

Los Jagueyes. This source was most common in the Rio Sta Maria sites because it occurs as a secondary deposit of obsidian along the Rio and distributaries (Shackley 2005:82-83). The source collection was from the INEGI Malpais H13A72 1:50,000 quadrangle. Abundant artifacts were noted including basin metates, and Cienega style projectile points, very similar to those in this collection (see cover image). No ceramics were located suggesting a Late Archaic occupation. Given that the study area was also an archaeological site, it is difficult to know whether all the obsidian marekanites collected were geological or archaeological. Furthermore, it is important to emphasize here that this "source area" is a secondary deposit. The primary source(s) is, as yet, unlocated, but given that some of the obsidian nodules were up to 50 mm in maximum diameter, it is likely not too distant.

Sierra Fresnal. The Sierra Fresnal is mainly composed of a series of coalesced rhyolite domes, some of which quenched at the outer margins during the eruptive event to produce obsidian (see Shackley 2005:83, Figure 3.15). The obsidian is eroding east into Lago Fresnal and Lago Guzman, and likely to the west as well (see Shackley 2005:Figure 3.15). Sierra Fresnal obsidian has been recovered in secondary deposits as well at Arroyo Seco south of Nuevo Casas Grandes and at Lago Fredrico. The Lago Fredrico obsidian collected by Alan Phelps exhibit slightly different elemental composition, but still similar, not unusual in obsidian derived from these large coalesced dome events (see Shackley 2005).

Agua Fria/Sierra la Breña. Agua Fria and Sierra la Breña are located nearby each other near the town of Agua Fria, Sonora, Agua Fria on the Sonoran side and Sierra la Breña over the state line on the Chihuahuan side (see Figure 1). The elemental composition of these sources collected independently by John Douglas and John Roney are statistically overlapping (see Shackley 2005: Tables A.12 and A.13). The distance between the sources is approximately 40 km, and it does appear that the Agua Fria source is likely secondary deposits eroded from Sierra la Breña (Shackley 2005:79-82). The author has not visited these sources. Nevertheless, the location is accurate, and as mentioned above suggests a procurement range that included the Sierra Madre seasonally or periodically.

Unknown sources. There are probably two, as yet, unlocated sources in the assemblage (see Figures 2 and 3). Northwest Mexico is somewhat *terra incognita* for obsidian sources at this time. There are certainly many sources yet unlocated that seem to appear in archaeological contexts in the region, some of which have been slowly located over the years (Fralik et al. 1998; Kibler et al. 2104; Shackley 1989, 1995, 2005).

Table 1. Elemental concentrations and probable source assignments for the archaeological obsidian, and RGM-1 a USGS rhyolite/obsidian standard. All measurements in part per million (ppm).

XRF #	Site/Project	Ti	Mn	Fe	Zn	Rb	Sr	Y	Zr	Nb	Ba	Pb	Th	Source
1	RSM-I	1602	737	22206	386	306	11	144	881	116	32	76	16	unknown
2	RSM-I	1700	865	26250	401	277	12	138	1293	115	29	66	19	Los Jagueyes
3	RSM-I	1543	951	27673	412	288	15	151	1376	119	0	73	19	Los Jagueyes
4	RSM	1804	995	30387	467	293	13	150	1395	114	68	68	21	Los Jagueyes
5	RSM-II	1489	837	26219	292	279	11	154	1442	129	0	57	25	Los Jagueyes
6	RSM-II	1564	954	28241	318	289	14	157	1469	130	0	66	34	Los Jagueyes
7	RSM-II	1354	922	26968	295	274	11	155	1583	134	0	58	23	Los Jagueyes
8	RSM-II	1650	812	23857	285	252	15	144	1421	117	0	52	30	Los Jagueyes
9	RSM-II	1605	821	25624	324	280	14	145	1391	124	0	62	26	Los Jagueyes
10	RSM-II	1207	351	9506	50	220	72	28	132	23	439	22	24	Agua Fria/Sierra la Breña
11	RSM-II	1512	953	27554	302	283	15	155	1485	127	0	67	29	Los Jagueyes
12	RSM-II	1661	388	11670	90	200	110	41	211	11	1310	25	27	Agua Fria/Sierra la Breña
13	RSM-II	2087	797	23660	307	244	12	137	1276	116	7	53	27	Los Jagueyes
14	RSM-I	1351	696	22734	375	282	12	145	1094	100	0	60	19	Los Jagueyes
15	RSM-I	1338	809	24277	342	268	9	138	1308	124	0	62	27	Los Jagueyes
16	RSM-I	1503	843	25039	327	267	14	147	1339	117	0	59	37	Los Jagueyes
17	RSM-I	1551	965	27835	364	295	13	154	1426	129	0	67	39	Los Jagueyes
18	RSM-I	1474	791	23811	382	262	13	140	1296	116	0	65	21	Los Jagueyes
19	PEÑON DEL DIABLO	1444	782	23618	367	326	14	141	875	118	0	77	31	unknown
20	RSM-I	1782	1045	31014	439	306	14	166	1556	141	0	64	47	Los Jagueyes
21	RSM-I	1451	892	26921	332	282	16	147	1405	122	0	60	26	Los Jagueyes
22	RSM	1553	887	25761	292	283	11	152	1439	128	0	58	17	Los Jagueyes
23	RSM-I	1724	852	26586	399	273	9	145	1318	114	0	60	19	Los Jagueyes
24	RSM-I	1457	784	23193	447	234	13	125	1169	106	0	54	25	Los Jagueyes
25	RSM-II	1235	745	22040	295	298	13	146	940	115	0	71	36	unknown
26	RSM-II	1562	941	27415	329	279	9	151	1450	131	0	65	12	Los Jagueyes
27	RSM-II	1523	359	11257	78	211	95	29	209	22	1236	22	18	Agua Fria/Sierra la Breña
28	RSM-II	1538	891	26415	306	280	9	145	1393	119	0	65	31	Los Jagueyes
29	RSM-II	1313	339	10362	58	252	60	40	181	29	376	19	51	Agua Fria/Sierra la

															Breña
30	RSM-I		1370	876	26233	310	282	9	154	1463	128	0	62	30	Los Jagueyes
31	RSM-II		1474	890	26877	327	282	16	149	1437	127	0	59	22	Los Jagueyes
32	RSM-I		4346	831	23990	372	238	12	136	1247	111	0	49	30	Los Jagueyes
XRF #	Site/Project		Ti	Mn	Fe	Zn	Rb	Sr	Y	Zr	Nb	Ba	Pb	Th	Source
33	RSM-I		1628	877	26052	381	309	15	142	892	121	7	71	30	unknown
34	RSM-II		4630	579	50067	184	206	253	15	211	14	794	31	4	unknown
35	RSM-II		1460	594	28719	360	282	12	190	1910	166	0	59	27	Los Jagueyes
36	RSM-I		1622	946	27822	367	284	10	151	1481	127	0	62	30	Los Jagueyes
37	RSM-I		1394	816	24693	279	271	11	146	1388	126	0	60	23	Los Jagueyes
38	RSM-I		1270	726	23146	270	295	14	158	1234	127	0	64	36	Los Jagueyes
39	RSM-I		1012	274	11919	69	286	36	63	161	23	124	30	45	Sierra Fresnal
40	RSM-I		1181	323	9143	62	201	56	27	165	28	500	20	26	Agua Fria/Sierra la Breña
41	RSM-I		1295	684	21142	271	301	14	140	908	117	0	65	36	unknown
42	RSM-I		1535	336	10781	79	197	103	31	198	16	1176	21	23	Agua Fria/Sierra la Breña
43	RSM-I		1710	762	22108	371	227	12	124	1157	111	36	48	24	Los Jagueyes
44	RSM-I		1433	891	25980	349	271	12	141	1410	127	10	64	29	Los Jagueyes
45	RSM-I		1505	582	28638	365	282	9	191	1896	166	15	57	44	Los Jagueyes
46	RSM-I		1568	848	26954	303	288	9	154	1450	130	0	67	38	Los Jagueyes
47	RSM-I		1339	805	24559	282	284	12	147	1442	125	0	55	22	Los Jagueyes
48	RSM-I		1472	868	26132	349	287	14	152	1394	133	0	61	41	Los Jagueyes
49	RSM-I		1392	844	25409	330	269	11	140	1358	131	0	54	27	Los Jagueyes
50	RSM-I		1920	812	24133	286	257	11	148	1345	124	0	61	26	Los Jagueyes
51	RSM-I		1219	267	12449	75	301	38	66	153	29	136	30	41	Sierra Fresnal
52	RSM-II		1365	766	24261	303	262	11	144	1370	114	0	57	25	Los Jagueyes
53	RSM-I		1669	782	23902	330	253	14	134	1319	117	0	54	27	Los Jagueyes
54	RSM-I		1478	252	11273	120	264	35	57	143	20	158	36	46	Sierra Fresnal
55	RSM-I		1151	683	20768	291	295	10	144	891	118	0	70	33	unknown
56	RSM-I		1644	390	11655	106	206	99	29	196	15	1127	25	22	Agua Fria/Sierra la Breña
57	RSM-II		1497	695	21700	296	271	11	135	1098	117	0	53	27	Los Jagueyes
58	RSM-I		1920	363	11047	72	200	107	32	210	16	1213	20	13	Agua Fria/Sierra la Breña
59	RSM-I		1068	289	12827	103	289	36	62	159	26	119	28	50	Sierra Fresnal
60	PEÑON	DEL	1392	825	20849	216	344	14	125	1189	102	0	41	30	unknown

61	DIABLO PEÑON DIABLO	DEL	2055	1123	34117	419	349	15	201	1946	150	0	64	44	Los Jagueyes
RGM1-S4			1526	295	13121	40	145	108	28	218	13	813	24	15	standard
RGM1-S4			1506	291	13099	43	143	109	26	212	7	824	21	17	standard
RGM1-S4			1566	299	13049	42	147	103	29	215	19	851	18	10	standard
RGM1-S4			1582	283	13194	47	148	104	27	221	14	856	22	24	standard

Table 2. Crosstabulation of obsidian source provenance by site/project from the data in Table 1.

			Source				
			Los Jagueyes	Agua Fria/Sierra la Breña	Sierra Fresnal	unknown	Total
Site/Project	PEÑON DEL DIABLO	Count	1	0	0	2	3
		% within Site/Project	33.3%	0.0%	0.0%	66.7%	100.0%
		% within Source	2.4%	0.0%	0.0%	25.0%	4.9%
		% of Total	1.6%	0.0%	0.0%	3.3%	4.9%
	RSM (unspecified)	Count	2	0	0	0	2
		% within Site/Project	100.0%	0.0%	0.0%	0.0%	100.0%
		% within Source	4.9%	0.0%	0.0%	0.0%	3.3%
		% of Total	3.3%	0.0%	0.0%	0.0%	3.3%
	RSM-I	Count	25	4	4	4	37
		% within Site/Project	67.6%	10.8%	10.8%	10.8%	100.0%
		% within Source	61.0%	50.0%	100.0%	50.0%	60.7%
		% of Total	41.0%	6.6%	6.6%	6.6%	60.7%
	RSM-II	Count	13	4	0	2	19
		% within Site/Project	68.4%	21.1%	0.0%	10.5%	100.0%
		% within Source	31.7%	50.0%	0.0%	25.0%	31.1%
		% of Total	21.3%	6.6%	0.0%	3.3%	31.1%
Total		Count	41	8	4	8	61
		% within Site/Project	67.2%	13.1%	6.6%	13.1%	100.0%
		% within Source	100.0%	100.0%	100.0%	100.0%	100.0%
		% of Total	67.2%	13.1%	6.6%	13.1%	100.0%

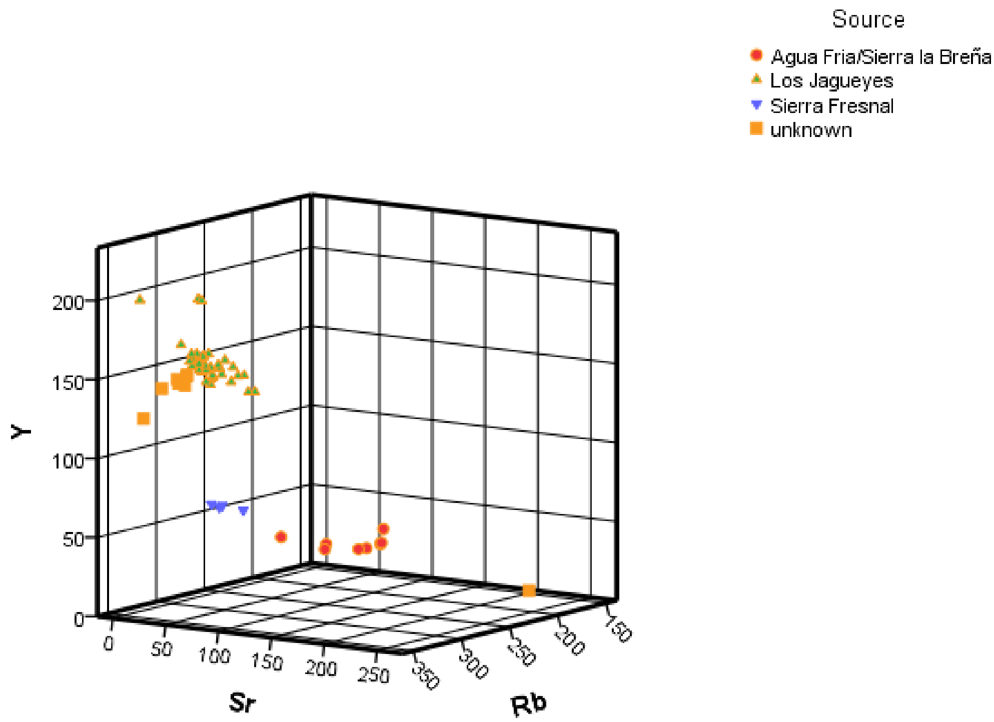

Figure 2. Sr/Y/Rb three-dimensional plot of the archaeological specimens. See Figure 2 for further discrimination. All measurements in parts per million (ppm).

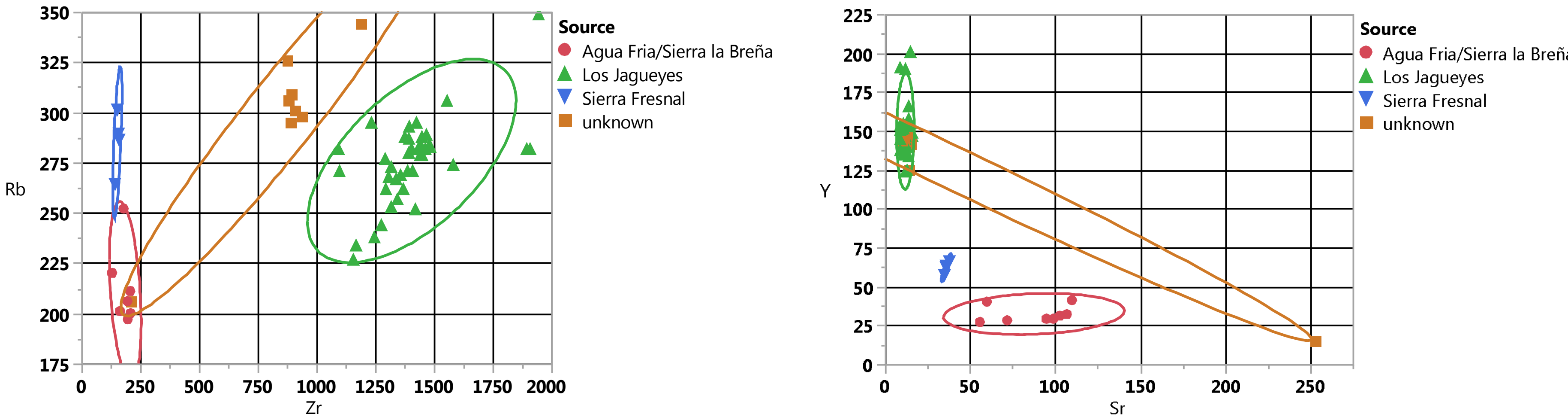

Figure 3. Zr/Rb and Sr/Y bivariate plots of the archaeological samples. All measurements in parts per million (ppm). Confidence ellipses at 95%. The overlap between Agua Fria/Sierra la Breña and unknown sample XRF #34 in the Zr/Rb plot is resolved with Sr. This unknown sample exhibits the highest Sr value in the assemblage.

References Cited

Davis, M.K., T.L. Jackson, M.S. Shackley, T. Teague, and J. Hampel
2011 Factors Affecting the Energy-Dispersive X-Ray Fluorescence (EDXRF) Analysis of Archaeological Obsidian. In *X-Ray Fluorescence Spectrometry (XRF) in Geoarchaeology*, edited by M.S. Shackley, pp. 45-64. Springer, New York.

Fralik, P.W. J.D. Stewart, and A.C. MacWilliams
1998 Geochemistry of West-Central Chihuahua Obsidian Nodules and Implications for the Derivation of Obsidian Artefacts. *Journal of Archaeological Science* 25:1023-1038.

Govindaraju, K.
1994 1994 Compilation of Working Values and Sample Description for 383 Geostandards. *Geostandards Newsletter* 18 (special issue).

Hampel, Joachim H.
1984 Technical Considerations in X-ray Fluorescence Analysis of Obsidian. In *Obsidian Studies in the Great Basin*, edited by R.E. Hughes, pp. 21-25. Contributions of the University of California Archaeological Research Facility 45. Berkeley.

Hildreth, W.
1981 Gradients in Silicic Magma Chambers: Implications for Lithospheric Magmatism. *Journal of Geophysical Research* 86:10153-10192.

Hughes, Richard E., and Robert L. Smith
1993 Archaeology, Geology, and Geochemistry in Obsidian Provenance Studies. *In Scale on Archaeological and Geoscientific Perspectives*, edited by J.K. Stein and A.R. Linse, pp. 79-91. Geological Society of America Special Paper 283.

Kibler, K.W., H.R. Hinojosa-Prieto, M.S. Shackley, and H.J. Hinojosa-García
2014 The Selene Obsidian Source (Formerly Sonora Unknown B) of the Upper Rio Bavispe Basin, Sonora, Mexico. *Kiva* 80: 168-192.

Mahood, Gail A., and James A. Stimac
1990 Trace-Element Partitioning in Pantellerites and Trachytes. *Geochemica et Cosmochimica Acta* 54:2257-2276.

McCarthy, J.J., and F.H. Schamber
1981 Least-Squares Fit with Digital Filter: A Status Report. In *Energy Dispersive X-ray Spectrometry*, edited by K.F.J. Heinrich, D.E. Newbury, R.L. Myklebust, and C.E. Fiori, pp. 273-296. National Bureau of Standards Special Publication 604, Washington, D.C.

Schamber, F.H.
1977 A Modification of the Linear Least-Squares Fitting Method which Provides Continuum Suppression. In *X-ray Fluorescence Analysis of Environmental Samples*, edited by T.G. Dzubay, pp. 241-257. Ann Arbor Science Publishers.

Shackley, M. Steven
1988 Sources of Archaeological Obsidian in the Southwest: An Archaeological, Petrological, and Geochemical Study. *American Antiquity* 53:752-772.

1989 *Early Hunter-Gatherer Procurement Ranges in the Southwest: Evidence from Obsidian Geochemistry and Lithic Technology*. Ph.D. dissertation, Department of Anthropology, Arizona State University, Tempe.

1995 Sources of Archaeological Obsidian in the Greater American Southwest: An Update and Quantitative Analysis. *American Antiquity* 60:531-551.

2005 *Obsidian: Geology and Archaeology in the North American Southwest*. University of Arizona Press, Tucson.

2011 An Introduction to X-Ray Fluorescence (XRF) Analysis in Archaeology. In *X-Ray Fluorescence Spectrometry (XRF) in Geoarchaeology*, edited by M.S. Shackley, pp. 7-44. Springer, New York.

Sliva, R. Jane
2015 *Projectile Points of the Early Agricultural Southwest: Typology, Migration, and Social Dynamics from the Sonoran Desert to the Colorado Plateau.* Desert Archaeology, Inc., Tucson, Arizona.